The magnetic torque of the heavy-fermion system UPd_2Al_3

1996 J. Phys.: Condens. Matter 8 729

(http://iopscience.iop.org/0953-8984/8/6/013)

J. Phys.: Condens. Matter **8** (1996) 729–740. Printed in the UK

The magnetic torque of the heavy-fermion system UPd_2Al_3

S Süllow†, B Janossy‡, G L E van Vliet†, G J Nieuwenhuys†, A A Menovsky†§ and J A Mydosh†

† Kamerlingh Onnes Laboratory, Leiden University, Leiden, The Netherlands

‡ High Magnetic Field Laboratory, Max-Planck-Institut für Festkörperforschung/Centre National de la Recherche Scientifique, Grenoble, France

§ Van der Waals–Zeeman Laboratory, University of Amsterdam, Amsterdam, The Netherlands

Received 15 September 1995, in final form 6 November 1995

Abstract. The basal-plane anisotropy of the antiferromagnetic phase of the hexagonal heavy-fermion superconductor UPd_2Al_3 has been studied via the magnetic torque. Torque measurements were performed as functions of magnetic field and angle, with the field rotated in the *a*–*b*-plane, at temperatures between 4.2 and 30 K and in fields of up to 20 T. We interpret our results within a mean-field model and derive expressions for the basal-plane anisotropy energy. Further, we studied the anisotropy and temperature dependence of the metamagnetic transition of UPd_2Al_3 at 18 T and we discuss its nature.

1. Introduction

In recent years research on heavy-fermion superconductors (HFS) has been, due to their uncommon physical properties, one of the major topics in low-temperature solid-state physics (for a review see [1]). The general opinion is that in these systems both superconductivity and magnetism are carried by the same strongly hybridized f electrons, unlike in the situation that we encounter in the case of the well-understood magnetic superconductors like RRh_4B_4 [2] and the newly discovered borocarbide systems [3, 4]. The former give rise to a multitude of magnetic and superconducting anomalies, and several theoretical models have been tried in an effort to explain these phenomena. Nevertheless, a thorough understanding of the physical properties of HFS and a firm theoretical description are still lacking. The major problem here is that the six of heavy-fermion superconductors currently known exhibit such a variety of different effects that they cannot be classified according to a distinct scheme.

One of the HFS exhibiting some extraordinary features is UPd_2Al_3 [5–10]. In this system, with hexagonal $PrNi_2Al_3$ structure, superconductivity coexists with antiferromagnetic ordering. It has the highest superconducting transition temperature of all the HFS ($T_c = 2$ K), and becomes antiferromagnetic below $T_N = 14.5$ K. Although the magnetic ordering temperature of UPd_2Al_3 is typical for the HFS, the magnitude of the ordered moment is not. While for other HFS the ordered magnetic moment amounts to about (0.01–0.1) μ_B, it is 0.85 μ_B in UPd_2Al_3 [11], which is large even for conventional magnetic U heavy-fermion systems.

Further, UPd_2Al_3 is one of the few U systems for which a crystalline-electric-field (CEF) scheme could be derived [12]. With this CEF scheme and by applying a molecular-field

0953-8984/96/060729+12$19.50

calculation, the bulk properties and the anisotropy between the hexagonal plane and the c axis of UPd_2Al_3 can be described consistently.

One open question about the physics of UPd_2Al_3 concerns the presence of a spin-wave energy gap. From transport measurements the existence of such a gap was inferred, with an energy of 20–40 K [13, 14, 15]. However, in inelastic neutron experiments no gap has been seen within the experimental resolution of about 4 K [16].

Another unsolved problem for UPd_2Al_3 is the nature of the metamagnetic transition at about 18 T. Different models for explaining this transition have been proposed: (i) a CEF-induced transition [17, 18], assuming that in high magnetic fields the CEF scheme is altered; (ii) a spin-flip process induced by the field at the transition from the antiferromagnetic to the high-field state [6]; and (iii) the breaking of the heavy-fermion state with a ferromagnetic ground state forming in high magnetic fields [9, 19].

In order to clarify the problems of the spin-wave energy gap and the metamagnetic transition, we have measured the magnetic torque of UPd_2Al_3 by rotating the field in the hexagonal basal plane. In this configuration the torque probes the anisotropy energy K_6^6 of the basal plane, and gives the scale of the energy gap of the magnon spectrum. The anisotropy energy K_6^6 was, within a mean-field approach, determined to be 3 mK, leading to a comparatively small value of 4.5 K of the spin-wave energy gap. Further, in the field dependence of the torque at the metamagnetic transition we find a drastic change of the absolute torque signal. This can only be accounted for by strong changes in the basal-plane anisotropy, and we interpret this as evidence that the CEF scheme is altered at the meta-magnetic transition.

2. Experimental techniques

The experiments were performed using the single crystal previously investigated by de Visser *et al* [6, 20, 21], and details regarding its production are described in the references. From the crystal a small piece was cut, with spatial dimensions of $2 \times 1 \times 0.5$ mm (with a mass of about 4 mg) and was checked by x-ray Laue diffraction for the orientation. The long axis of the crystal was oriented along the crystallographic c axis, with a misorientation $\leqslant 5^\circ$. Additionally the a and b axes were indexed, with similar misorientations. While the a axis denotes a unit-cell vector ($\langle 100 \rangle$), the b axis does not. With the b axis the direction $\langle 110 \rangle$ in the unit cell is assigned and spans an angle of 30° with the a axis (note that with the sixfold degeneracy of the basal plane further b axis vectors are found at 90° and 150° with respect to a particular chosen a axis). This convention is illustrated in figure 1. Here, both the structure of the basal plane of UPd_2Al_3 with the assignment of the a and b axes (figure 1(a)) as well as the unit cell of UPd_2Al_3 in the hexagonal supercell (figure 1(b)) are shown. The arrows on the U atoms illustrate the structure of the magnetic ordering in zero magnetic field with a wave vector $\boldsymbol{q} = (\frac{1}{2}00)$ [11].

The torque experiments were performed in Grenoble and in Leiden. In the experiments we employed a spring torque meter, with the torque measured as the capacitance between a metallic spring (Cu–Be or Cu–P), on which the sample is mounted, and the ground plate. In Grenoble at the High Magnetic Field Laboratory of the MPI/CNRS torque was measured as function of the magnetic field, with the field, which was swept up and down again, oriented at different angles in the hexagonal a–b-plane at temperatures between 4.2 and 30 K. For measurements below 15 T the sample was mounted on a soft spring (upper limit of exertable torque force $\approx 10^{-5}$ N m), together with a coil for calibration. For measurements up to 20 T a much stiffer spring (usable up to 10^{-3} N m) without a calibration coil was employed.

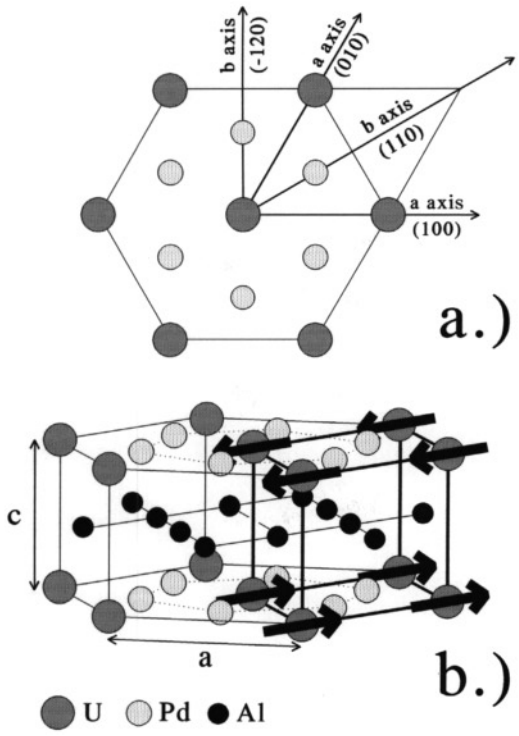

Figure 1. (a) The structure of the hexagonal basal plane of UPd_2Al_3 with the assignment of the a and b axes, as used in the text. (b) The crystallographic unit cell of UPd_2Al_3, which crystallizes in the $PrNi_2Al_3$ structure, together with the hexagonal supercell. The arrows on the U atoms in the unit cell show the magnetically ordered structure in zero magnetic field for a wave vector $\boldsymbol{q} = (\frac{1}{2}\,0\,0)$.

Absolute values of the magnetic torque were obtained by normalizing the data for the stiff spring to the data for the soft one (the relative error of the stiff spring data is about $\pm 10\%$). The direction of the torque sensor in the field (and thus the direction of the field in the hexagonal plane) could be changed via a mechanical screw. With this mechanism no angular sweep at fixed field could be done, but only field sweeps at fixed angle. In Leiden at the Kamerlingh Onnes Laboratory the torque set-up was built into a rotatable resistive magnet and the torque measured as a function of field orientation in the basal plane at fixed fields up to 1.1 T at 4.2 K. Here also no calibration coil was used, and absolute values were derived by comparison with the data taken in Grenoble (relative accuracy about $\pm 10\%$).

3. Results

The torque exerted on a sample is $\boldsymbol{\tau} = \boldsymbol{m} \times \boldsymbol{B} = mB \sin\Theta = m_\perp B$, with Θ the angle between the total magnetic moment $\boldsymbol{m}$ of the sample and the magnetic field $\boldsymbol{B}$, and $m_\perp$ the component of $\boldsymbol{m}$ perpendicular to $\boldsymbol{B}$. In an ideal isotropic system the torque is zero at all fields, since the magnetization is always aligned along the field direction. Torque is caused by anisotropy, and measures the misalignment of the magnetization with respect to the magnetic field. If the torque is zero in an anisotropic system for a particular field direction at all fields, this denotes a symmetry axis of the system. If no hysteresis is visible

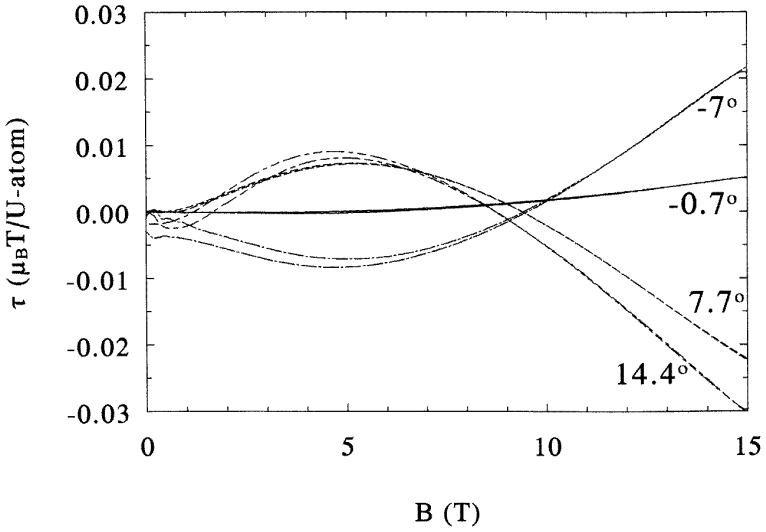

Figure 2. The field dependence of the magnetic torque τ of UPd_2Al_3 below 15 T for field orientations close to the *b* axis. The degree notations mark the angle between the magnetic field for each particular measurement and the *b* axis.

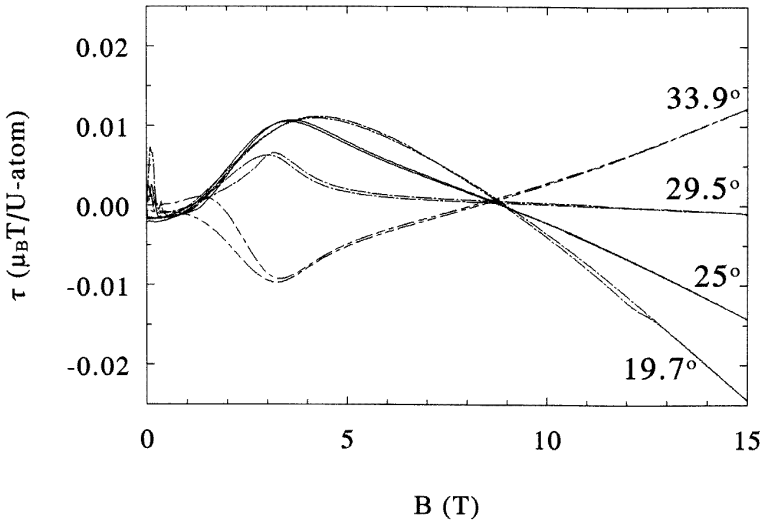

Figure 3. The field dependence of the magnetic torque τ of UPd_2Al_3 below 15 T for field orientations close to the *a* axis.

in the torque as the field is rotated through the symmetry axes, it marks the easy magnetic axis. However, in assigning easy and hard magnetic axis, one must bear in mind that in a simple antiferromagnet the spins are oriented perpendicular to the field direction, while in a ferro- and paramagnet they are parallel. Further, in real magnetic systems magnetic domain formation has to be taken into consideration. In general, domains will reduce the measured magnetic torque.

In figures 2 and 3 the magnetic torques τ in fields below 15 T at 4.2 K for different

field orientations are shown. Each measurement is labelled by the angle between the field and the *b* axis. The presence of magnetic torque in the antiferromagnetic phase immediately implies anisotropy in the *a*–*b*-plane. The angular dependence of the field sweeps shows a symmetric behaviour. With the field oriented close to the *b* axis (0.7°, figure 2) τ is nearly zero; as soon as the field is rotated away from the *b* axis a characteristic torque pattern with a hysteretic maximum and subsequently a change of sign at 9 T arises, with opposite absolute values for opposite field positions relative to the *a* and *b* axes.

The absolute values of τ for all field directions are quite small; the effective perpendicular magnetic moment $m_\perp$ exerting the torque is of the order of hundreds of μ_B. The general shape of the torque slightly changes with the orientation of the magnetic field in the basal plane. When the field is within 20° of the *b* axis, the torque anomaly is rather broad with its maximum positioned at about 5 T, but it appears more like a kink for fields aligned close to the *a* axis with the peak just above 3 T. For lowest fields the torque is quite irregular and strongly hysteretic, especially for fields close to the *a* axis (figure 3). This is due to the presence of magnetic domains in this field range [12].

The *a* axis is the easy magnetic axis, since with the field directed along the *b* axis the moments are mainly directed along the *a* axis in the case of antiferromagnetic ordering (figure 2). Here, with τ being zero, the moments are in their equilibrium positions. On the other hand, with the field oriented close to the *a* axis the moments have to rotate close to the *b* axis (figure 3). In this case the presence of the hysteretic anomaly proves this spin position to be a nonequilibrium state. This result is in agreement with statements of other groups [8, 22].

More information about the low-field torque can be obtained by measurements as a function of angle. In figure 4 we plot the result of our measurements, with the magnetic field $B \leqslant 1.1$ T rotated in the basal plane at angles between $-55°$ and 55° with respect to the *b* axis. As can be seen, at a certain field (0.77 T) a periodic pattern arises with a periodicity of 60°. This is due to the basal-plane anisotropy in the system. The higher the field, the more regular the pattern appears, implying that—especially at low fields—τ is affected by magnetic domains. At 1.1 T the domains have only minor influence on the shape of the pattern (the maximum values of the torque at 1.1 T at $-20°$ and 40° slightly differ, but the reason for this is that we did not correct the torque data for the sample holder contribution, which, however, is small). The torque smoothly changes sign when the field is rotated through the *b* axis—while hysteretic torque, again with a change of sign, is observed for the field-rotated through the *a* axis, similar to what we observed in the field-dependent torque measurements presented above.

The angular dependence of the torque is governed by the spins rotating in the basal plane. If the field is aligned parallel to the *b* axis (0°), then τ is zero. Increasing the angle between the *b* axis and the magnetic field increases the torque, because the moments oriented along the *a* axis (their equilibrium state) try to keep their alignment and, accordingly, give rise to an average magnetic moment $m_\perp$. When the field crosses the *a* direction the spins rotate through the *b* axis; a reorientation of spins becomes more favourable, and after their hysteretic motion over the potential barrier, they drop into the next potential minimum (*a* axis) leading to the change of sign of the torque.

Figure 5 shows the metamagnetic transition at about 18 T as seen in torque for two directions of the field with respect to the *b* axis. The absolute values of τ ($m_\perp$) are about 30 (20) times larger above the metamagnetic transition than in the low-field regime (which made it necessary to use the stiffer torque sensor). The torque τ above the transition continues to increase, and the magnetic moment $m_\perp$ therefore remains nearly constant. This indicates considerable anisotropy in this field range. The metamagnetic transition

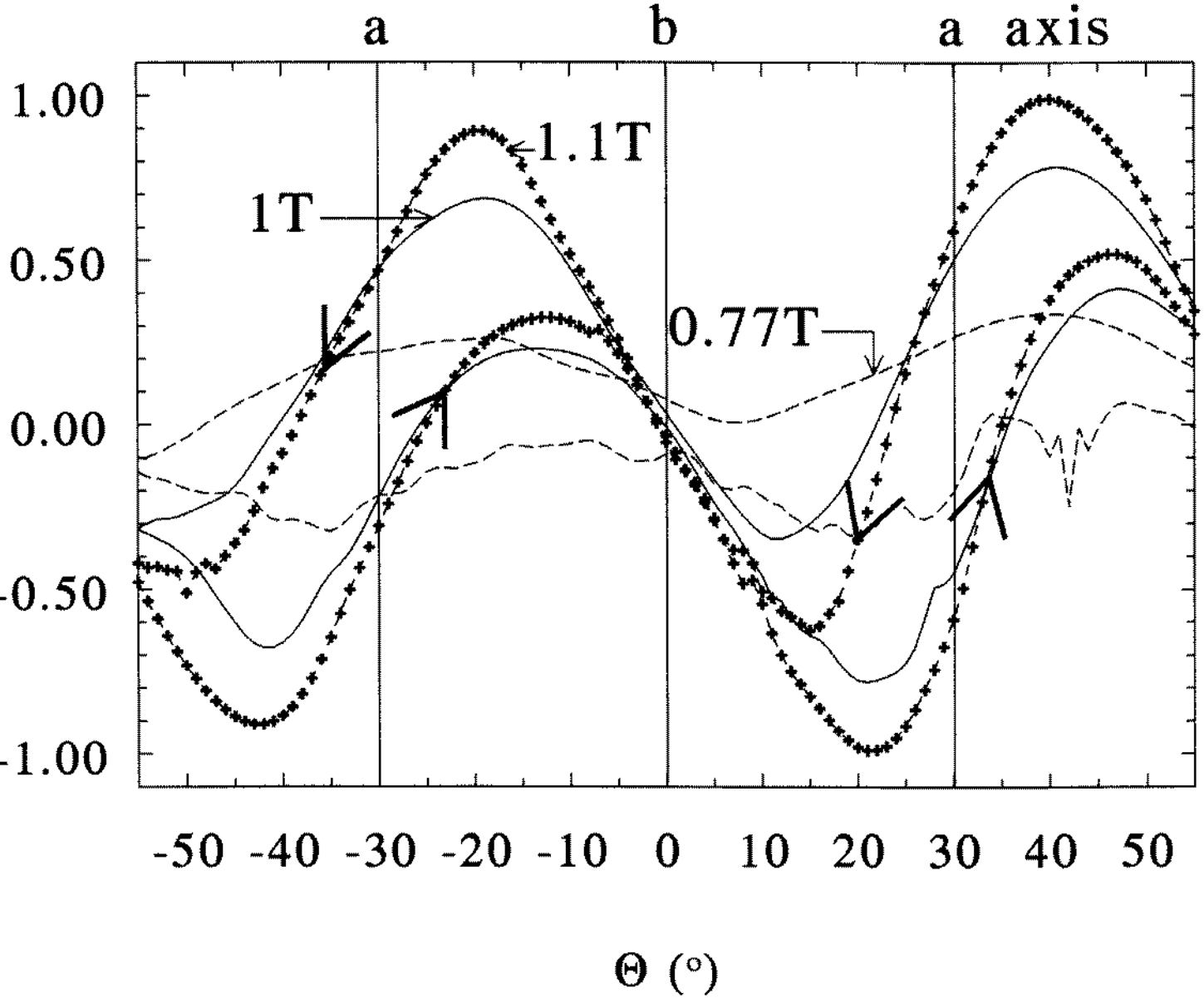

Figure 4. The angular dependence of the magnetic torque τ of UPd_2Al_3. Measurements are performed at fields of 1.1 T (– + –), 1 T (—) and 0.77 T (– –). The arrows indicate the direction of the angular sweep in the measurement.

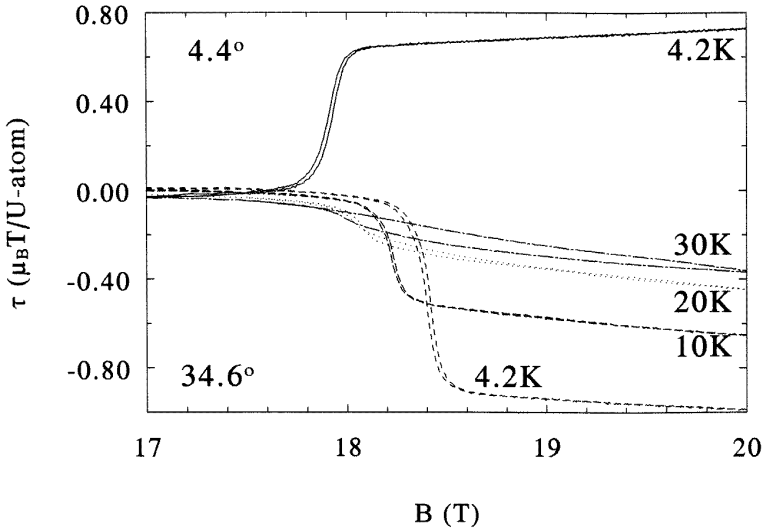

Figure 5. The metamagnetic transition of UPd_2Al_3 as seen for a field-dependent magnetic torque τ for two different directions. The upwards-directed transition has been taken at an angle of 4.4° from the *b* axis, and the downwards-directed transition at an angle of 34.6°, at temperatures denoted in the plot.

itself appears as a sharp, but hysteretic jump with an angle-dependent transition field. This anisotropy has already been established in [9, 19, 21], although these studies on the anisotropy of the metamagnetic transition are inconsistent regarding one particular point. In [9, 19] the minimum in the metamagnetic transition field is reported to appear in the case of the magnetic field oriented close to the *a* axis. In contrast, in [21] the opposite situation is found with the minimum transition field visible for fields aligned along the *b* axis. Our measurements support the latter data of de Visser *et al* [21]. Further, we find that the metamagnetic transition persists at temperatures above $T_N = 14.5$ K and smears with increasing temperature. This is in good agreement with previous reports [9, 19], even though in those measurements of the linear magnetization the transition at higher temperatures appeared as a much broader feature. Similarly to the low-field anomalies, the high-field transition changes sign with the field rotated through the *a* or *b* axis, so in total an 'upwards'-directed bump (i.e. the torque anomaly below 9 T) in the low-field torque is commensurate with an 'upward' jump at the metamagnetic transition and vice versa.

4. Discussion

In our discussion we will consider two points in detail: first, we will give a qualitative and semi-quantitative interpretation of the low-field torque measurements within a mean-field approximation. Second the metamagnetic transition is treated within a similar mean-field approach leading to a qualitative explanation for the huge change of torque at the transition.

The magnetic torque τ of a spin system can be calculated if the angle between the average magnetic spin moment $\boldsymbol{m}$ of the system and the magnetic field $\boldsymbol{B}$ is known. This moment $\boldsymbol{m}$ can be determined by minimizing the energy E_{spin} of the spin system for given $\boldsymbol{B}$ and given local spin potentials. There are three contributions to the spin energy E_{spin}.

The first is the energy E_B of the magnetic field. For a single spin this is

$$E_B = -MB\cos(\Theta_B - \Theta_m) \tag{1}$$

with M the magnitude of the magnetic moment m in units of μ_B, B the magnetic field in tesla and Θ_B and Θ_m the angles the magnetic field and the magnetic moment span with an arbitrary coordinate axis. In our case the problem can be simplified, since the spins are restricted to the hexagonal a–b-plane, and $\boldsymbol{B}$, also, is oriented in the basal plane. Therefore, we choose the reference axis, against which the angles Θ_B and Θ_m are measured, to be the b axis.

From the angle-dependent torque measurements (figure 4) it is obvious that the spins rotate in the basal plane in a potential of sixfold symmetry. This can be taken into account via a single-spin anisotropy energy E_6

$$E_6 = k_B K_6^6 \cos(6\Theta_m) \tag{2}$$

with k_B the Boltzmann factor and the anisotropy K_6^6 measured in kelvin. Note that a positive value for K_6^6 indicates that the a axis is the easy axis.

Finally, we must take into account the antiferromagnetic ordering in UPd_2Al_3. The appropriate energy E_{AFM} cannot be treated as a single-spin energy, but is the interaction energy of two neighbouring spins. We approximate this energy as

$$E_{AFM} = k_B J\cos(\Theta_{m1} - \Theta_{m2}) \tag{3}$$

with J as the magnetic interaction measured in kelvin, and Θ_{m1} and Θ_{m2} as the angles of two antiferromagnetically coupled spins measured with respect to the b axis. Combining these terms we obtain the expression for the average single-spin energy as a function of the position of two spins m_1 and m_2:

$$E_{spin}(m_1, m_2) = \frac{1}{2}\left[E_B(m_1) + E_B(m_2) + E_6(m_1) + E_6(m_2)\right] + E_{AFM}. \tag{4}$$

This expression for the spin energy, can, for given M, B, K_6^6, J and Θ_B, be minimized with respect to the angle of the spins Θ_{m1} and Θ_{m2}. The values of M (0.85 μ_B for UPd_2Al_3), B and Θ_B are determined experimentally, and the free parameters are K_6^6 and J.

Although the model used here to describe the spin energy is the simplest we could devise, and we cannot account for domain effects, and have neither included the temperature dependence of the problem (T = 0 K) nor the possible dependence of the parameters K_6^6 and J on magnetic field (magnetostrictive effects), it accounts for the major features that we observe in our low-field torque measurements. With the minimization of E_{spin} we can determine for K_6^6 and J values of 3 mK and 5 K, respectively, and thereby qualitatively and semi-quantitatively describe our field and angular dependence of the torque measurements. Typical results are given in figures 6 and 7.

In figure 6 we plot the calculated torque of UPd_2Al_3 with $K_6^6 = 3$ mK and $J = 5$ K as a function of field for different angles with respect to the b axis. The main properties of the measurements—that is, the torque anomaly with the shape and maximum changing from a broad bump to a kink while the field is rotated from the b to the a axis and the sign reversal of τ at 9 T—reproduce well. The absolute values of τ above 9 T are in good agreement with the measured data. At lower fields the calculated values are two to three times larger than the measured ones, and the field of the maximum of τ appears somewhat lower in the calculation than in the experiment. On the other hand, the hysteresis is more pronounced in the measurements, although, in the calculation, hysteresis is also found at the low-field anomaly. The stronger experimental hysteresis at low fields is predominantly caused by the magnetic domains.

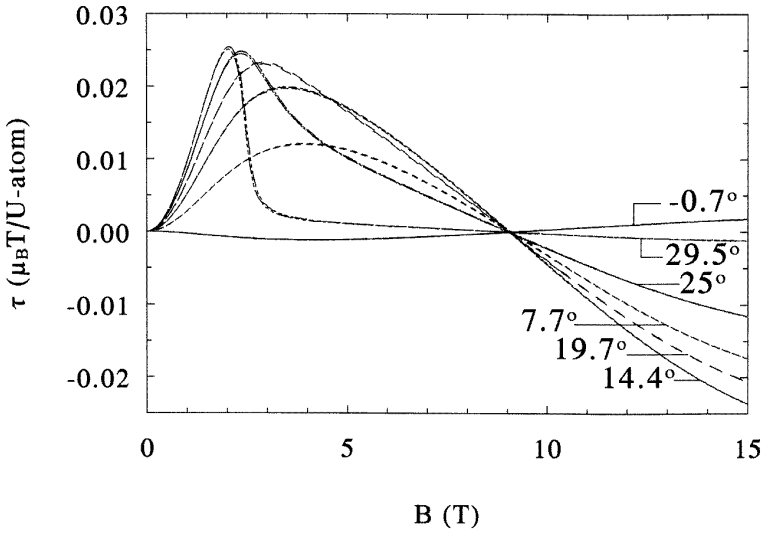

Figure 6. The field dependence of the calculated magnetic torque τ of UPd_2Al_3 below 15 T for different field orientations, according to the model described in the text. The parameter values used are $K_6^6 = 3$ mK and $J = 5$ K.

In figure 7 the calculated torque as function of angle at fixed fields up to 2 T is plotted. Here again the primary effect of a hysteretic spin flop along the a axis above a certain field reproduces well in the model calculation. In our calculation the absolute values of the torque are again larger than the measured data, and the spin flop appears at a somewhat higher field (for the given choice of parameters it is observable above 1.5 T). In part, this is due to magnetic domain effects, which are strong at low fields, lowering the observed torque and broadening the characteristic features. In addition, the low-field torque is affected by spin waves, as we will indicate below, and this also reduces the measured torque.

It has been shown by Coqblin [23], that in hexagonal symmetry, for spins ferromagnetically coupled in the a–b-plane and antiferromagnetically coupled along the c axis, the gap in the spin-wave spectrum can be written as

$$\Delta = 12\sqrt{\frac{1}{2}K_6^6 P_2} \tag{5}$$

with K_6^6 the anisotropy parameter as derived above, and P_2 as the second-order parameter in the crystalline-electric-field Coqblin Hamiltonian. The parameter can be expressed in terms of the Stevens operators:

$$P_2 = 3B_2^0 + (25 - 30S(S+1))B_4^0 + +(105S^2(S+1)^2 - 525S(S+1) + 294)B_6^0. \tag{6}$$

The values of B_i^0 have been reported for UPd_2Al_3 by Böhm *et al* [24]: $B_2^0 = 8.74$ K, $B_4^0 = 57.5$ mK and $B_6^0 = 3.10$ mK for $S = 4$. These numbers lead to $P_2 = 91.7$ K, and with $K_6^6 = 3$ mK we finally arrive at $\Delta = 4.5$ K as the gap in the spin-wave spectrum. Due to the coarseness of our approach, this value of Δ gives only the order of magnitude of the gap. Still, it is obvious that this gap is extraordinarily small, and at a measurement temperature of 4.2 K a large number of spin waves will be thermally excited. These magnons will affect the torque such that absolute values will be lowered and the anomalies arising from the motion of the spins over the potential barriers in the basal plane be broadened.

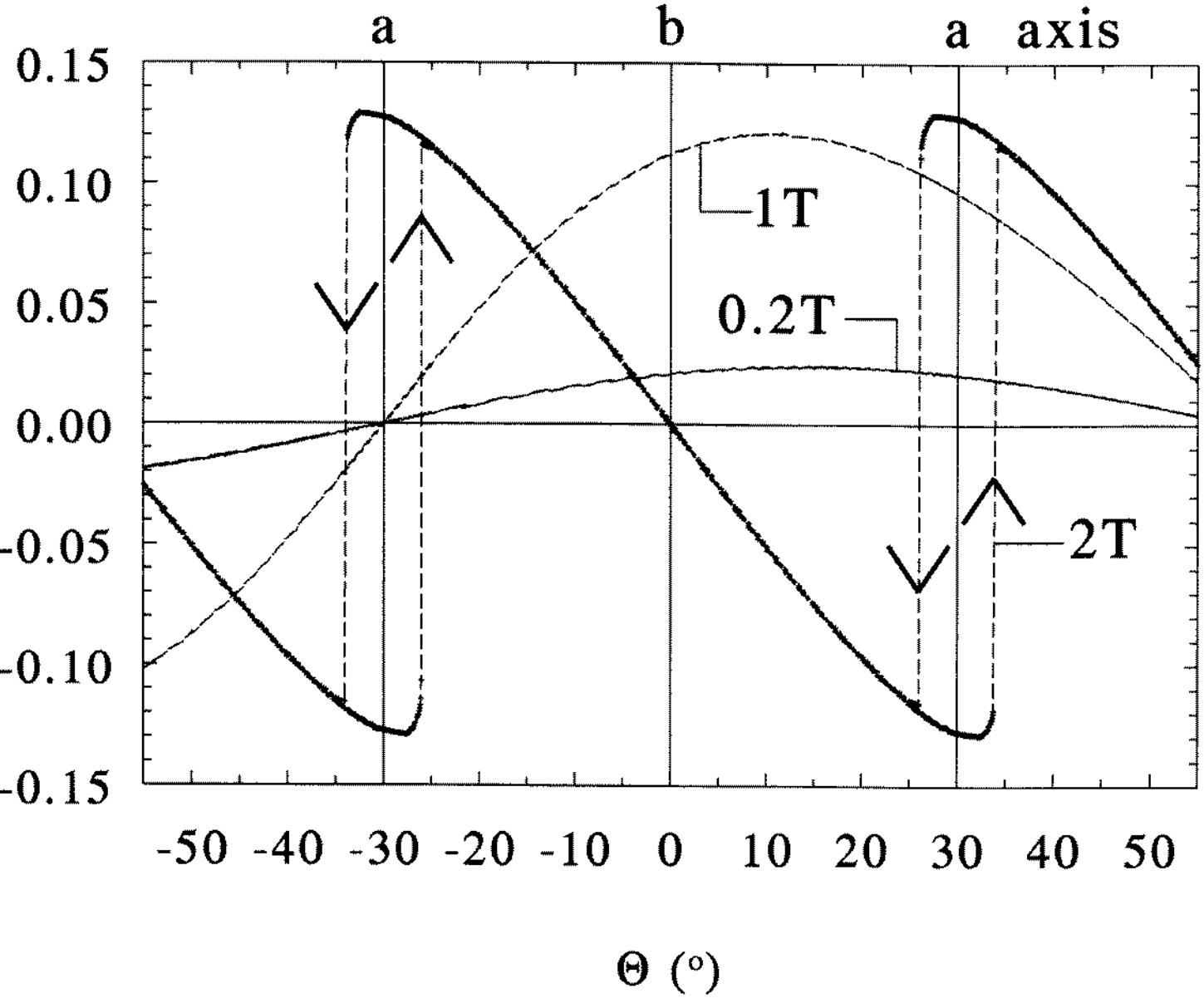

Figure 7. The calculated angular dependence of the magnetic torque τ of UPd_2Al_3. The calculations were performed for fields of 0.2 T (—), 1 T (– –), and 2 T (– + –). The arrows indicate the direction of the angular sweep in the calculation.

With this taken into account, it appears that our $T = 0$ K model will result in torque values that are too high, if compared to measurements for low fields at temperatures of the same order as the magnon energy gap. On the other hand, in high magnetic fields thermal excitations will be less important, since the thermal energy is only a portion of the total magnetic energy of the spin system, and thus the agreement between the model and experiment will be better. Further, we remark that the small value of Δ explains why no magnon energy gap has been seen in inelastic neutron scattering [16]. The resolution in the experiment was too low to allow for a direct determination of the gap.

The above mean-field calculation can also be employed to examine the metamagnetic transition at 18 T. However, now we cannot use the same parameters as for the low-field state. In particular, from our torque measurements we cannot deduce whether the magnetic exchange J above the transition is ferro-, antiferro- or paramagnetic, since these different appearances of magnetism are indistinguishable in torque, and therefore, in principle, we have to discuss the three cases independently. Fortunately, the situation can be simplified. First, we note that at 18 T the magnetic torque generated by an anisotropic ferromagnet hardly differs from that of an anisotropic paramagnetic system; in both cases the spins are oriented close to the field direction, and the misalignment creating the torque is generated solely by the anisotropy. Thus, we can treat the ferromagnetic and the paramagnetic case as one. Secondly, linear magnetization experiments [6, 9, 19] show at the metamagnetic transition a jump-like increase of the magnetization from 0.6 to 1.5 μ_B/U atom, a feature which cannot be explained by assuming that the high-field state is again one of antiferromagnetic ordering.

Consequently, above the metamagnetic transition we can restrict ourselves to considering only the case of paramagnetic spins ($J = 0$) with moments of 1.5 μ_B in an anisotropic potential, with freedom to choose K_6^6. We remark that, since above the transition the direction of the easy magnetic axis might have changed, K_6^6 can be either positive or negative, corresponding to the a or b axis being the easy axis. If now we minimize the spin energy E_{spin} from equation (4), we find that, in order to reproduce the angular dependence and the absolute values of the high field the torque as well as the change of sign of torque at the transition, we have to assume that K_6^6 is negative (thus the b axis is the easy axis) with an absolute value of the order of 0.1–0.2 K. Hence, in spite of the simplicity of our approach, we find that above the transition the strength of the anisotropy is substantially increased, and even the direction of the easy magnetic axis has changed, if compared to the low-field antiferromagnetic phase. This we take as a strong indication that at the metamagnetic transition a change in the CEF levels takes place leading to a different anisotropy. This conclusion is supported by the fact that the metamagnetic transition is also observed for temperatures above T_N.

5. Conclusion

In summary, we performed magnetic torque measurements to study the basal-plane anisotropy of the antiferromagnetic and high-field phases of the heavy-fermion superconductor UPd_2Al_3. The low-field torque behaviour could be qualitatively and semi-quantitatively explained within a simple mean-field model. In particular, we could derive an expression for the basal-plane anisotropy energy K_6^6, which turned out to be rather small (3 mK) compared to the antiferromagnetic exchange interaction J (=5 K). Based on K_6^6 we could estimate the energy gap in the spin-wave spectrum ($\Delta = 4.5$ K). Due to the small value of the energy gap a large number of magnons will be excited at the measurement temperatures, and this, together with magnetic domain effects, reconciles the

differences between our calculations and the measurements. Further, it explains the lack of any signature of a magnon energy gap in inelastic neutron scattering measurements [16]. Within a similar mean-field model we studied the metamagnetic transition at 18 T, which yielded a qualitative insight into the nature of this transition. Here, we found that the basal-plane anisotropy is strongly altered at the transition and that the magnetic 5f moment is increased. These results favour an explanation of the metamagnetic transition as being induced by a CEF.

Acknowledgments

We thank E Steep and G Goll for their assistance during the measurements. We thank Professor R P Griessen for his advice on building the 'Leiden' torque meter. This work was partially supported by the Nederlandse Stichting voor Fundamenteel Onderzoek der Materie (FOM). The samples were prepared at FOM–ALMOS.

References

[1] Hess D W, Riseborough P S and Smith J L 1993 *Encyclopedia of Applied Physics* vol 7 (New York: VCH) p 35
[2] See, e.g.,
Fischer Ø and Maple M B (ed) 1982 *Superconductivity in Ternary Compounds I* (Berlin: Springer)
[3] Cava R J, Takagi H, Batlogg B, Zandbergen H W, Krajewski J J, Peck W F Jr, van Dover R B, Felder R J, Siegrist T, Mizuhashi K, Lee J O, Eisaki H, Carter S A and Uchida S 1994 *Nature* **367** 148
[4] Cava R J, Takagi H, Zandbergen H W, Krajewski J J, Peck W F Jr, Siegrist T, van Dover R B, Felder R J, Mizuhashi K, Lee J O, Eisaki H and Uchida S 1994 *Nature* **367** 252
[5] Geibel C, Schank C, Thies S, Kitazawa H, Bredl C D, Böhm A, Rau M, Grauel A, Caspary R, Helfrich R, Ahlheim U, Weber G and Steglich F 1991 *Z. Phys.* B **84** 1
[6] de Visser A, Nakotte H, Tai L T, Menovsky A A, Mentink S A M, Nieuwenhuys G J and Mydosh J A 1992 *Physica* B **179** 84
[7] Caspary R, Hellmann P, Keller M, Sparn G, Wassilew C, Köhler R, Geibel C, Schank C, Steglich F and Phillips N E 1993 *Phys. Rev. Lett.* **71** 2146
[8] Kita H, Dönni A, Endoh Y, Kakurai K, Sato N and Komatsubara T 1994 *J. Phys. Soc. Japan* **63** 726
[9] Oda K, Kumada T, Sugiyama K, Sato N, Komatsubara T and Date M 1994 *J. Phys. Soc. Japan* **63** 3115
[10] Feyerherm R, Amato A, Gygax F N, Schenck A, Geibel C, Steglich F, Sato N and Komatsubara T 1994 *Phys. Rev. Lett* **73** 1849
[11] Krimmel A, Fischer P, Roessli B, Maletta H, Geibel C, Schank C, Grauel A, Loidl A and Steglich F 1992 *Z. Phys.* B **86** 161
[12] Grauel A, Böhm A, Fischer H, Geibel C, Köhler R, Modler R, Schank C, Steglich F, Weber G, Komatsubara T and Sato N 1992 *Phys. Rev.* B **46** 5818
[13] Dalichaouch Y, de Andrade M C and Maple M B 1992 *Phys. Rev.* B **46** 8671
[14] Bakker K, de Visser A, Tai L T, Menovsky A A and Franse J J M 1993 *Solid State Commun.* **86** 497
[15] Huth M, Kaldowski A, Hessert J, Steinborn T and Adrian H 1993 *Solid State Commun.* **87** 1133
[16] Petersen T, Mason T E, Aeppli G, Ramirez A P, Bucher E and Kleiman R N 1994 *Physica* B **199+200** 151
[17] Mentink S A M 1994 *PhD Thesis* Leiden University
[18] Konno R 1994 *J. Phys. Soc. Japan* **63** 3442
[19] Sugiyama K, Inoue T, Oda K, Kumada T, Sato N, Komatsubara T, Yamagishi A and Date M 1994 *Physica* B **201** 227
[20] de Visser A, Bakker K, Tai L T, Menovsky A A, Mentink S A M, Nieuwenhuys G J and Mydosh J A 1993 *Physica* B **186–188** 291
[21] de Visser A, van der Meulen H P, Tai L T and Menovsky A A 1994 *Physica* B **199+200**
[22] Paolasini L, Paixão J A, Lander G H, Burlet P, Sato N and Komatsubara T 1994 *Phys. Rev.* B **49** 7072
[23] Coqblin B 1977 *The Electronic Structure of Rare-Earth Metals and Alloys* (London: Academic)
[24] Böhm A, Grauel A, Sato N, Schank C, Geibel C, Komatsubara T, Weber G and Steglich F 1993 *Int. J. Mod. Phys.* B **7** 34